7. Y. Haupt, S. Rowan, E. Shaulian, K. Vousden, M. Oren, *Genes Dev.* **9**, 2170 (1995); C. Ishioka *et al.*, *Oncogene* **10**, 1485 (1995).
8. pBabepuro p53ER^{TM} or DN-p53ER^{TM} was transfected into PA317 retroviral packaging cells. Recombinant retrovirus harvested at 48 hours was used to infect VSMCs, rat 1 fibroblasts, or MEFs in polybrene (8 μg/ml). Cells were selected in puromycin (2.5 μg/ml) and resistant cells were pooled.
9. T. Littlewood, D. Hancock, P. Danielian, M. Parker, G. Evan, *Nucleic Acids Res.* **23**, 1686 (1995).
10. M. Bennett, T. Littlewood, S. Schwartz, P. Weissberg, *Circ. Res.* **81**, 591 (1997).
11. S. Yonehara, A. Ishii, M. Yonehara, *J. Exp. Med.* **169**, 1747 (1989); N. Itoh *et al.*, *Cell* **66**, 233 (1991).
12. Cells (1×10^6) were incubated with CH-11 (20 μg/ml) for 30 min on ice followed by a secondary fluorescein isothiocyanate–conjugated anti-mouse IgG (Sigma). Total Fas expression was analyzed by permeabilizing cells in ethanol for 30 min before Fas staining. Higher expression of cytoplasmic compared with surface Fas was evident in rat and human fibroblasts, mesangial cells, and rat VSMCs, but not in THP-1 or HeLa cells.
13. R. Klausner, J. Donaldson, J. Lippincott-Schwartz, *J. Cell Biol.* **116**, 1071 (1992); M. Ladinsky and K. Howell, *Eur. J. Cell Biol.* **59**, 92 (1992).
14. DN-p53(302–370) encodes the oligomerization domain of p53 [E. Shaulian, A. Zauberman, D. Ginsberg, M. Oren, *Mol. Cell. Biol.* **12**, 5581 (1992)].
15. R. Watanabe-Fukunaga, C. I. Brannan, N. G. Copeland, N. A. Jenkins, S. Nagata, *Nature* **356**, 314 (1992); T. Takahashi *et al.*, *Cell* **76**, 969 (1994).
16. A. Chinnaiyan, K. O'Rourke, M. Tewari, V. Dixit, *Cell* **81**, 505 (1995). DN-FADD [(FADD(80–208)] contains the death domain of FADD and therefore binds Fas, but lacks the NH_2-terminal death effector domain required for apoptosis.
17. C. A. Ray *et al.*, *Cell* **69**, 597 (1992); M. Tewari and V. Dixit, *J. Biol. Chem.* **270**, 597 (1995); K. Smith, A. Strasser, D. Vaux, *EMBO J.* **15**, 5167 (1996).
18. Time-lapse videomicroscopy examined the course of 100 randomly selected cells over 24 hours. Cumulative apoptotic deaths at 4-hour intervals were plotted against time. Mean deaths for each time point and experimental condition for a minimum of three independent experiments are given. Videomicroscopic measurements of apoptosis were confirmed against trypan blue exclusion (a measure of loss of viability).
19. Mouse anti-Fas IgG (10 μg/ml) was bound to protein G–Sepharose (1 hour, 4°C). p53ER^{TM} VSMC lysates were incubated with anti-Fas–protein G complexes (3 hours, 4°C), precipitated, separated by 10% SDS–polyacrylamide gel electrophoresis (PAGE) in nonreducing conditions, and blotted with mouse anti-human FADD IgG (1 μg/ml).
20. p53ER^{TM} VSMCs (5×10^6) were incubated in nocodazole (10 μg/ml) and latrunculin A (5 μg/ml) in 10 mM Hepes (pH 7.4) for 30 min at 37°C. The cell sediment was first swollen with 150 mM KCl, 10 mM tris-acetate-EDTA (pH 7.4) for 10 min on ice, washed twice in KEHM [150 mM KCl, 10 mM EGTA, 50 mM Hepes-KOH (pH 7.4), 2 mM $MgCl_2$], and protease inhibitor cocktail (PIC, Sigma), resuspended in an equal volume of KEHM, and homogenized. The homogenate was centrifuged through a discontinuous sucrose gradient (1.6, 1.2, or 0.8 M sucrose in KEHM and PIC), and the Golgi-enriched fraction was collected from the 0.8/1.2 M sucrose interface, separated by 10% SDS-PAGE, blotted, and probed with mouse anti-Fas IgG (100 ng/ml) (#F22120, Transduction Labs). Fractions were compared against homogenate, and whole-cell lysate was isolated for protein immunoblots.
21. Retroviruses encoding pBabe Hygro FADD-DN or control vector (pBabe Hygro) [A. O. Hueber *et al.*, *Science* **278**, 1305 (1997)] were synthesized as in (*10*), cells were selected in hygromycin (200 μg/ml), and resistant cells were pooled.
22. A Nru–Dra III fragment from pcDNA3 crmA (*16*), cloned into the adenovirus shuttle plasmid pAdBglII, was cotransfected with Xba I–Cla I–digested sub360 genomic DNA [T. Ohno *et al.*, *Science* **265**, 781 (1994)] into 293 cells. Recombinant virus was isolated by plaque purification, propagated in 293 cells, and purified by caesium chloride centrifugation. Virus titers were determined by plaque assay. Target cell infection of 100% was obtained with a multiplicity of infection of 100 per cell.
23. We thank R. Hicks for flow cytometry, T. Littlewood for pBabe p53ER^{TM}, E. Nabel and G. Nabel for crmA adenovirus, D. Galloway for pLHPV-E6 type 16, A. Hueber for *lpr* and *gld* MEFs and pBabe DN-FADD, T. Suganuma for anti-galactosyl transferase, and F. Buss, G. Evan, and M. Oren for advice and comments.
Supported by British Heart Foundation grants FS/97024, PG/95057, and PG/96040 (to M.B.) and CH/9400 (to P. W.), Medical Research Council grant G9310915 (to J.P.L.), and NIH grant HL34073 and the Bruce and Ruth Rappaport Program in Vascular Biology (to R.S.).

7 April 1998; accepted 4 September 1998

Bifurcation of Lipid and Protein Kinase Signals of PI3Kγ to the Protein Kinases PKB and MAPK

Tzvetanka Bondeva,* Luciano Pirola,* Ginette Bulgarelli-Leva, Ignacio Rubio, Reinhard Wetzker, Matthias P. Wymann†

Phosphoinositide 3-kinases (PI3Ks) activate protein kinase PKB (also termed Akt), and PI3Kγ activated by heterotrimeric guanosine triphosphate–binding protein can stimulate mitogen-activated protein kinase (MAPK). Exchange of a putative lipid substrate-binding site generated PI3Kγ proteins with altered or aborted lipid but retained protein kinase activity. Transiently expressed, PI3Kγ hybrids exhibited wortmannin-sensitive activation of MAPK, whereas a catalytically inactive PI3Kγ did not. Membrane-targeted PI3Kγ constitutively produced phosphatidylinositol 3,4,5-trisphosphate and activated PKB but not MAPK. Moreover, stimulation of MAPK in response to lysophosphatidic acid was blocked by catalytically inactive PI3Kγ but not by hybrid PI3Kγs. Thus, two major signals emerge from PI3Kγ: phosphoinositides that target PKB and protein phosphorylation that activates MAPK.

PI3Ks play a central role in cell signaling and lead to cell proliferation and survival, motility, secretion, and specialized cell responses such as the respiratory burst of granulocytes (*1*). It is assumed that these responses are mediated by the major lipid product of the class I PI3K family, phosphatidylinositol 3,4,5-trisphosphate [PtdIns(3,4,5)P_3]. The protein kinase PKB is a direct target of PtdIns(3,4)P_2 (*2*) and is further activated by phosphoinositide-dependent kinases (PDKs) (*3*).

Heterodimeric p85/p110 PI3Kα and PI3Kγ both have protein kinase activity (*4*, *5*). Moreover, PI3Kα-mediated phosphorylation of its regulatory p85 subunit decreases the enzyme's lipid kinase activity (*4*). The functions of PI3K have often been established with the PI3K inhibitors wortmannin and LY294002 or with catalytically inactive PI3K constructs (*6*, *7*). Such manipulations interfere with both lipid and protein kinase activities of PI3Ks (*4*, *5*), and a physiological role of PI3K signaling through its protein kinase activity has not been established. We therefore engineered PI3Ks that allowed us to separately study the lipid and protein kinase activities of PI3Kγ.

A region within the conserved catalytic core of PI3Kγ (*8*) was replaced by the corresponding sequences of PI3Ks of class II (which phosphorylate PtdIns or PtdIns 4-*P* in vitro), class III (restricted to PtdIns), and FRAP [a member of the target of rapamycin family without assigned lipid kinase activity (Fig. 1A)]. The exchanged sequences correspond to the activation loop in cAMP-dependent protein kinase and insulin receptor tyrosine kinase and seem to regulate the access of PI substrates to the catalytic core (*9*). When expressed in 293 cells as glutathione-S transferase (GST)–PI3Kγ fusion proteins, purified wild-type PI3Kγ phosphorylated PtdIns, PtdIns 4-*P*, and PtdIns(4,5)P_2, whereas the hybrid of PI3Kγ with a class II insert (cII) phosphorylated only PtdIns and PtdIns 4-*P* (Fig. 1B). In vitro production of PtdIns 3-*P* by cII was equal to that of the wild-type enzyme (1.1-fold, ±0.1 SE, n = 3) in the absence of cholate and much greater than that of wild type in the presence of cholate (22.9-fold, ±2.7 SE, n = 5). The hybrid with a class III insert (cIII) behaved like the PtdIns 3-kinase involved in vacuolar protein sorting (Vps34p) and

T. Bondeva, I. Rubio, R. Wetzker, Research Unit "Molecular Cell Biology," University of Jena, D-07747 Jena, Germany. L. Pirola, G. Bulgarelli-Leva, M. P. Wymann, Institute of Biochemistry, University of Fribourg, CH-1700 Fribourg, Switzerland.

*These authors contributed equally to this work.
†To whom correspondence should be addressed. E-mail: MatthiasPaul.Wymann@UniFR.ch

phosphorylated PtdIns exclusively. Finally, the enzyme with the FRAP insert (cIV) did not phosphorylate lipids at all. Thus, the transferred sequences are sufficient to confer the donor protein's characteristic in vitro lipid specificity (*1*) to PI3Kγ. Although protein kinase activity was maintained in all hybrid proteins (cII through cIV), a PI3Kγ with a $Lys^{832} \rightarrow Arg$ mutation (*5*) was catalytically inactive (Fig. 2A).

Wortmannin reactivity was reduced for cIII (Fig. 2A) and was eliminated in the catalytically inactive PI3Kγ (*5*). However, the lipid kinase activity of the wild type and of cII and cIII hybrids was equally sensitive to wortmannin. Autophosphorylation of the FRAP-PI3Kγ hybrid (cIV) was completely abolished by 100 nM wortmannin (*10*). Incubation with the substrates adenosine triphosphate (ATP) and PtdIns(4,5)P_2 protected wild-type and hybrid proteins against covalent modification by wortmannin (Fig. 2C). Thus, hybrid proteins retain the properties of the wild-type PI3Kγ, such as inhibitor sensitivity, ATP binding, and protein kinase activity, but are restricted in their ability to phosphorylate PIs in vitro.

It has been proposed that serpentine receptor-mediated MAPK activation involves PI3Kγ-derived PtdIns(3,4,5)P_3 and that tyrosine phosphorylation of SHC initiates the SHC/Grb2/mSOS/Ras cascade (*11*). Expression of full-length untagged PI3Kγ and of cII, cIII, and cIV hybrids led to a three- to fivefold increase in MAPK activity in serum-starved COS7 cells. This increase was not observed when cells were first incubated with 100 nM wortmannin or in cells expressing catalytically inactive PI3Kγ (Fig. 3A). This demonstrates that a PI3Kγ-specific wortmannin-sensitive activity is required for MAPK activation. Because the only enzymatic activity common to wild-type and cII through cIV PI3Kγs is protein phosphorylation, this protein kinase activity apparently signals to MAPK.

Both PI3Kα and PI3Kγ interact with Ras (*12*). A PI3Kγ Ras-binding mutant (*13*) activated MAPK to a greater extent than did wild-type PI3Kγ (Fig. 3A). Thus, Ras-mediated translocation of PI3Kγ to the plasma membrane may be of minor importance for the activation of MAPK signaling. Furthermore, a comparison of untagged wild-type or hybrid PI3Kγs with PI3Kγs extended by a COOH-terminal isoprenylation signal of K-Ras (PI3Kγ-CAAX) revealed that only the soluble and protein kinase–active, but not membrane-attached, forms could activate MAPK (Fig. 3B). PI3Kγ-CAAX with the wild-type catalytic center, on the other hand, constitutively activated PKB in serum-starved COS7 cells (Fig. 3B), whereas catalytically inactive PI3Kγ-CAAX, cII through cIV PI3Kγ-CAAX, and all soluble forms had no effect.

We used metabolic labeling with ^{32}P-labeled inorganic phosphate and subsequent analysis of deacylated lipids on high-performance liquid chromatography (HPLC) to show that PtdIns(3,4)P_2 and PtdIns(3,4,5)P_3 were only produced in cells transfected with wild-type PI3Kγ-CAAX when cultivated without serum. No signal could be detected for the hybrids cII through cIV, as shown for cII (Fig. 3C). The correlation of PtdIns(3,4)P_2 and PtdIns(3,4,5)-P_3 production with PKB activation is in agreement with earlier reports on the lipid's effects on PDKs (*3*) and PKB itself (*2*). The fact that MAPK activation can be triggered in the complete absence of PtdIns(3,4)P_2 and

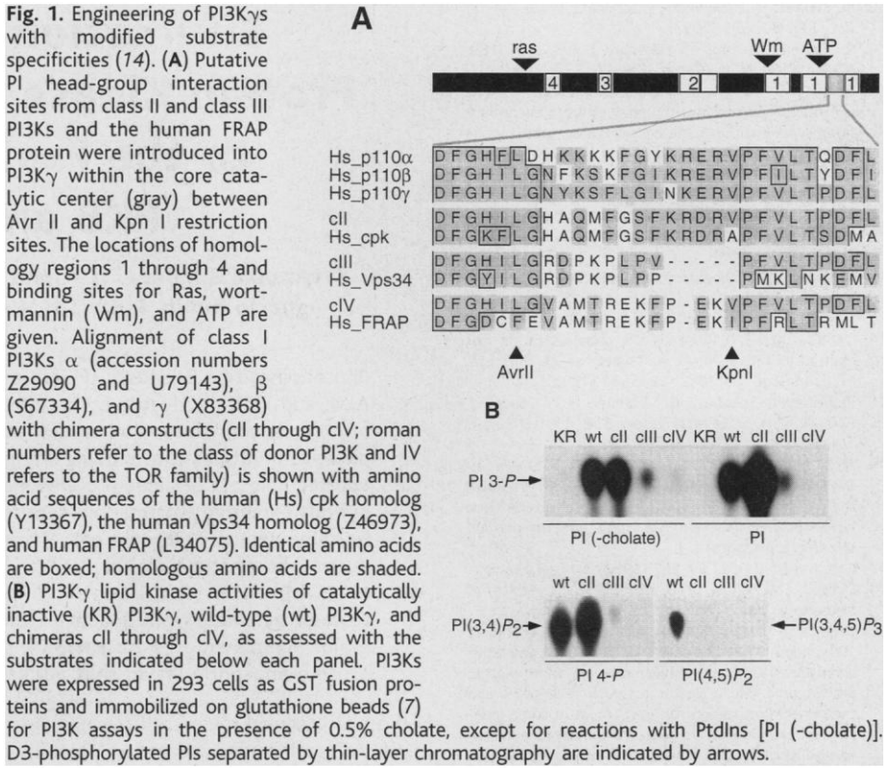

Fig. 1. Engineering of PI3Kγs with modified substrate specificities (*14*). (**A**) Putative PI head-group interaction sites from class II and class III PI3Ks and the human FRAP protein were introduced into PI3Kγ within the core catalytic center (gray) between Avr II and Kpn I restriction sites. The locations of homology regions 1 through 4 and binding sites for Ras, wortmannin (Wm), and ATP are given. Alignment of class I PI3Ks α (accession numbers Z29090 and U79143), β (S67334), and γ (X83368) with chimera constructs (cII through cIV; roman numbers refer to the class of donor PI3K and IV refers to the TOR family) is shown with amino acid sequences of the human (Hs) cpk homolog (Y13367), the human Vps34 homolog (Z46973), and human FRAP (L34075). Identical amino acids are boxed; homologous amino acids are shaded. (**B**) PI3Kγ lipid kinase activities of catalytically inactive (KR) PI3Kγ, wild-type (wt) PI3Kγ, and chimeras cII through cIV, as assessed with the substrates indicated below each panel. PI3Ks were expressed in 293 cells as GST fusion proteins and immobilized on glutathione beads (*7*) for PI3K assays in the presence of 0.5% cholate, except for reactions with PtdIns [PI (-cholate)]. D3-phosphorylated PIs separated by thin-layer chromatography are indicated by arrows.

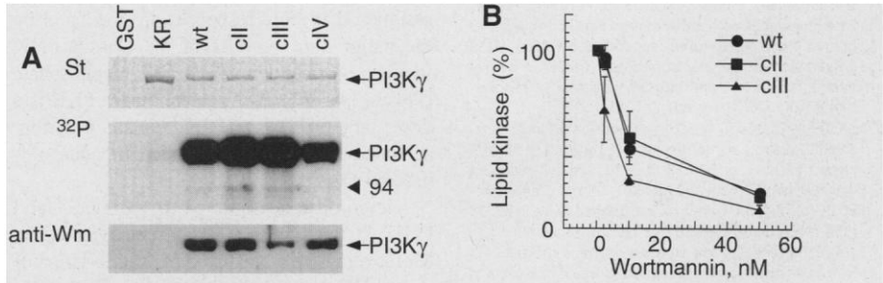

Fig. 2. Protein kinase activity and inhibitor and substrate interactions of PI3Kγ proteins. (**A**) GST-PI3Kγ fusion proteins as indicated (top) were expressed and isolated (Fig. 1) and quantitated by Coomassie blue staining (St). PI3Kγ protein kinase activities were monitored by autophosphorylation of PI3Kγ (^{32}P) as described (*5*). Covalent interaction of wortmannin with PI3Kγ and hybrids was detected by incubation of immobilized PI3Kγs with 100 nM wortmannin for 10 min at 0°C. Samples were denatured and subjected to SDS–polyacrylamide gel electrophoresis. Bound wortmannin was detected with antibodies to wortmannin (anti-Wm) (*7*). (**B**) Wortmannin inhibition of PtdIns phosphorylation. PI3Kγ was exposed to wortmannin at the concentrations indicated. A standard lipid kinase assay was done, and the data were normalized to the respective nontreated control (n = 3, mean ± SE). (**C**) PI3Kγs were incubated where indicated with 1 mM ATP or PtdIns(4,5)P_2 (PIP_2) (0.1 mg/ml) before wortmannin was added. Anti-Wm immunoblots were done as in (*7*).

PtdIns(3,4,5)P_3, and by the lipid kinase–deficient cIV construct, indicates that 3-phosphorylated PIs are not required for this process. Instead, PI3Kγ-associated protein kinase activity may be the mediator of MAPK activation. Moreover, a permanent attachment of PI3Kγ to the membrane seems to interfere with MAPK activation, which suggests that PI3Kγ must be liberated from the membrane to perform this function.

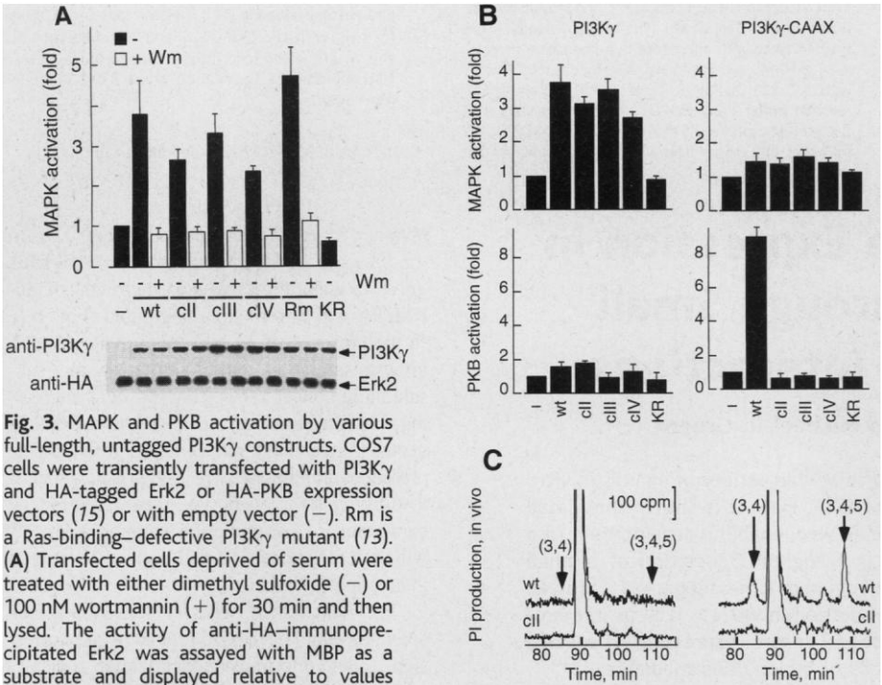

Fig. 3. MAPK and PKB activation by various full-length, untagged PI3Kγ constructs. COS7 cells were transiently transfected with PI3Kγ and HA-tagged Erk2 or HA-PKB expression vectors (*15*) or with empty vector (−). Rm is a Ras-binding–defective PI3Kγ mutant (*13*). (**A**) Transfected cells deprived of serum were treated with either dimethyl sulfoxide (−) or 100 nM wortmannin (+) for 30 min and then lysed. The activity of anti-HA–immunoprecipitated Erk2 was assayed with MBP as a substrate and displayed relative to values from cells transfected with Erk2 alone (n = 3, mean ± SE). The expression of PI3Kγ was probed with monoclonal antibody to PI3Kγ (anti-PI3Kγ), and the expression of Erk2 was probed with antibodies to HA (anti-HA). (**B**) PI3Kγ [left panels in (B) and (C)] and membrane-targeted PI3Kγ [PI3Kγ-CAAX; right panels in (B) and (C)] were tested for their potential to activate MAPK or PKB. MAPK activity was determined as in (A). PKB activation was assayed with a peptide substrate (*15*). Expression of PI3Kγ, Erk2, and PKB was equal in all experiments. ($n \geq 3$, mean ± SE). (**C**) Lipid kinase activities of wild-type PI3Kγ and cII substrate mutants in COS7 cells. Lipids were extracted from cells labeled with inorganic phosphate ($^{32}P_i$) deprived of serum, deacylated, and separated by HPLC (*6*). The elution times of the deacylation products of PtdIns(3,4)P_2 and PtdIns(3,4,5)P_3 are indicated by (3,4) and (3,4,5), respectively.

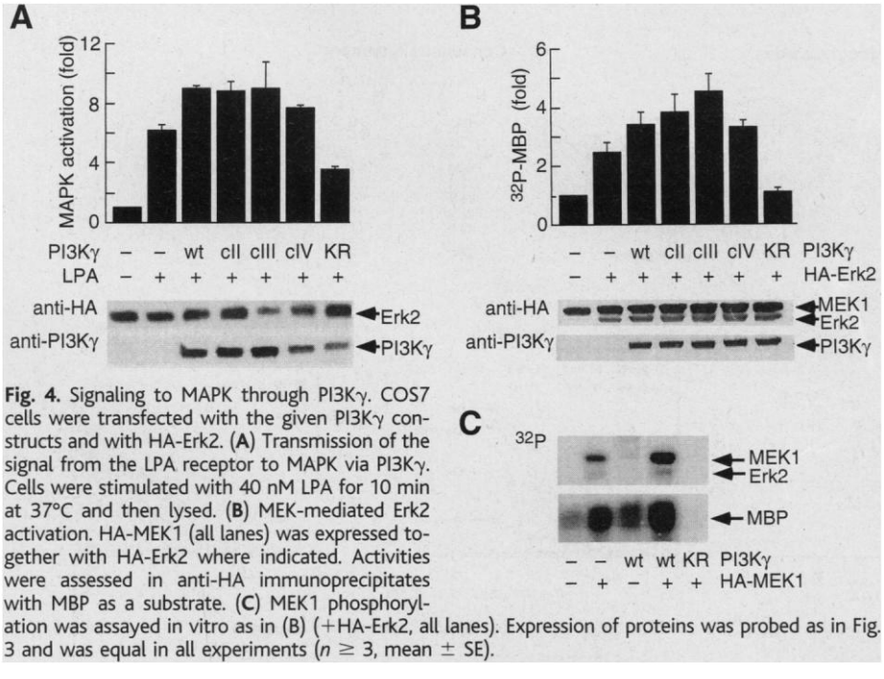

Fig. 4. Signaling to MAPK through PI3Kγ. COS7 cells were transfected with the given PI3Kγ constructs and with HA-Erk2. (**A**) Transmission of the signal from the LPA receptor to MAPK via PI3Kγ. Cells were stimulated with 40 nM LPA for 10 min at 37°C and then lysed. (**B**) MEK-mediated Erk2 activation. HA-MEK1 (all lanes) was expressed together with HA-Erk2 where indicated. Activities were assessed in anti-HA immunoprecipitates with MBP as a substrate. (**C**) MEK1 phosphorylation was assayed in vitro as in (B) (+HA-Erk2, all lanes). Expression of proteins was probed as in Fig. 3 and was equal in all experiments ($n \geq 3$, mean ± SE).

To investigate whether hybrid PI3Kγs are able to transmit signals from seven-transmembrane helix receptors, transfected COS7 cells were stimulated with lysophosphatidic acid (LPA). LPA triggered a six- to sevenfold increase in MAPK activity, which was further increased by wild-type and cII through cIV PI3Kγs. Catalytically inactive PI3Kγ inhibited the LPA-induced activation of MAPK (Fig. 4A).

MEK1, Erk2, and PI3Kγ constructs were expressed together to assess the influence of PI3Kγ on MEK1-mediated activation of MAPK. Immunoprecipitions of MEK1 showed a threefold increase in myelin basic protein (MBP) phosphorylation activity in cells that were also transfected with Erk2. All PI3Kγs with protein kinase activity further increased MBP phosphorylation (Fig. 4B). When catalytically inactive PI3Kγ was transfected instead, MBP phosphorylation was reduced to that seen in cells expressing MEK1 alone. These results indicate that the protein kinase activity of PI3Kγ may be required for the activation of Erk2/MAPK through MEK1. This is supported by the finding that phosphorylation of MEK1 in vitro is increased in immunoprecipitations from cells expressing wild-type PI3Kγ but is abolished in immunoprecipitations from cells expressing catalytically inactive PI3Kγ (Fig. 4C).

We conclude that PI3Kγ generates two distinct forward signals: 3-phosphorylated PIs that activate PKB and protein kinase activity that contributes to MAPK activation.

References and Notes

1. B. Vanhaesebroeck, S. J. Leevers, G. Panayotou, M. D. Waterfield, *Trends Biochem. Sci.* **22**, 267 (1997); A. Toker, and L. C. Cantley, *Nature* **387**, 673 (1997).
2. T. F. Franke, D. R. Kaplan, L. C. Cantley, A. Toker, *Science* **275**, 665 (1997); A. Klippel, W. M. Kavanaugh, D. Pot, L. T. Williams, *Mol. Cell. Biol.* **17**, 338 (1997).
3. D. R. Alessi *et al.*, *Curr. Biol.* **7**, 261 (1997); D. Stokoe *et al.*, *Science* **277**, 567 (1997); L. Stephens *et al.*, *ibid.* **279**, 710 (1998).
4. C. L. Carpenter *et al.*, *Mol. Cell. Biol.* **13**, 1657 (1993); R. Dhand *et al.*, *EMBO J.* **13**, 522 (1994).
5. S. Stoyanova *et al.*, *Biochem. J.* **324**, 489 (1997).
6. A. Arcaro and M. P. Wymann, *ibid.* **296**, 297 (1993).
7. M. P. Wymann *et al.*, *Mol. Cell. Biol.* **16**, 1722 (1996).
8. B. Stoyanov *et al.*, *Science* **269**, 690 (1995); L. R. Stephens *et al.*, *Cell* **89**, 105 (1997).
9. L. Pirola, G. Bulgarelli-Leva, M. Zvelebil, M. D. Waterfield, M. P. Wymann, in preparation.
10. L. Pirola and M. P. Wymann, unpublished data.
11. M. Lopez-Ilasaca, P. Crespo, P. G. Pellici, J. S. Gutkind, R. Wetzker, *Science* **275**, 394 (1997).
12. P. Rodriguez-Viciana *et al.*, *EMBO J.* **15**, 2442 (1996). I. Rubio *et al.*, *Biochem. J.* **326**, 891 (1997).
13. The Lys^{270} → Glu mutation in PI3Kγ, in analogy to the Lys^{227} → Glu Ras-binding mutant of PI3Kα by Rodriguez-Viciana *et al.* (*12*), reduced Ras binding by >80% (T. Bondeva, unpublished data).
14. PI3Kγ hybrids were generated by the introduction of synthetic oligonucleotides to replace PI3Kγ coding sequences between Avr I and Kpn I restriction sites (Fig. 1A). Manipulated regions were sequenced, subcloned into a cytomegalovirus promoter–driven expression

vector (pSTC-tkGST) (*7*), and transfected by the calcium phosphate method into 293 cells. In vitro kinase assays with immobilized proteins were done as described in (*6*).

15. COS7 cells were cultured in Dulbecco's modified Eagle's medium supplemented with fetal calf serum (10%). Subconfluent cells were transfected by the DEAE method with pcDNA3-based expression vectors (Invitrogen). The amount of plasmid DNA was kept constant by the addition of empty vector when necessary (2 μg per 10-cm plate). After 24 hours, cells were deprived of serum for 24 hours and subsequently treated with inhibitors or stimulated before lysis [in 20 mM Hepes (pH 7.5), 10 mM EGTA, 1% NP-40, 2.5 mM $MgCl_2$, 2 mM Na_3VO_4, 1 mM dithiothreitol, and 40 mM β-glycerophosphate, supplemented with 1 mM phenylmethylsulfonyl fluoride, aprotinin (20 μg/ml), and leupeptin]. Hemagglutinin (HA)-tagged Erk2, MEK1, and PKB were immunoprecipitated from the centrifuged lysates with mouse monoclonal antibodies to HA (anti-HA, 12CA5 from Babco) for 1 to 2 hours at 4°C and immobilized on Gamma-bind Sepharose (Pharmacia). Beads were washed twice with phosphate-buffered saline containing 1% NP-40 and 2 mM Na_3VO_4, followed by washes with 100 mM tris (pH 7.5) with 0.5 M LiCl and MAPK reaction buffer [12.5 mM MOPS (pH 7.5), 12.5 mM β-glycerophosphate, 7.5 mM $MgCl_2$, 0.5 mM EGTA, 0.5 mM NaF, and 0.5 mM Na_3VO_4]. Myelin basic protein was the substrate for Erk2 and MEK1; for PKB assays, crosstide peptide was used [R. Meier, D. R. Alessi, P. Cron, M. Andjelkovic, B. A. Hemmings, *J. Biol. Chem.* **272**, 30491 (1997)].

16. We thank K.-L. Guan for MEK, R. Marais for Raf, T. Franke for PKB expression plasmids, S. Gutkind for plasmids described in (*11*), B. Hemmings and R. Meier for help with the PKB assay and crosstide peptide, and A. Schneider for criticism. Supported by Swiss National Science Foundation grant 3100-50506.97 (to M.P.W.).

17 June 1998; accepted 9 September 1998

Controlling Gene Expression in Living Cells Through Small Molecule–RNA Interactions

Geoffrey Werstuck* and Michael R. Green†

Short RNA aptamers that specifically bind to a wide variety of ligands in vitro can be isolated from randomized pools of RNA. Here it is shown that small molecule aptamers also bound their ligand in vivo, enabling development of a method for controlling gene expression in living cells. Insertion of a small molecule aptamer into the 5′ untranslated region of a messenger RNA allowed its translation to be repressible by ligand addition in vitro as well as in mammalian cells. The ability of small molecules to control expression of specific genes could facilitate studies in many areas of biology and medicine.

In vitro genetic selections (*1*) have been used to isolate nucleic acid sequences (aptamers) that bind small molecules with high affinity and specificity (*2*). The ability to control gene expression by using cell-permeable small molecules offers several advantages, and small molecule manipulation of gene expression at the levels of transcription (*3*) and signal transduction (*4*) has been reported.

We selected RNA aptamers that specifically bound to the related aminoglycoside antibiotics kanamycin A and tobramycin (Fig. 1A) (*5*). We analyzed the ability of these aptamers to function in vivo by expressing them in *Escherichia coli* and testing for a drug-resistant phenotype (*6*). In the absence of drug, bacterial strains expressing no aptamer (bl-RSETA), the kanamycin aptamer (bl-kan1), or the tobramycin aptamer (bl-tob1) grew similarly (Fig. 1B). In the presence of 10 μM kanamycin A, bl-kan1 grew to saturation, whereas growth of bl-RSETA and bl-tob1 was negligible (Fig. 1C). In the presence of 10 μM tobramycin, bl-tob1 grew to saturation, and bl-kan1 grew to a subsaturating concentration (Fig. 1C) (*7*). Increasing the number of aptamers in the expression vector from one to three enhanced growth in the presence of antibiotic (Fig. 1D). Thus, a specific drug-resistant phenotype was conferred by expression of an aminoglycoside aptamer (*8*), which demonstrates a small molecule–aptamer interaction in vivo.

We next asked whether small molecule aptamers could be used to regulate gene expression. Eukaryotic translation initiation typically involves 5′-to-3′ scanning from the 5′-m^7G cap to the start codon (*9*). Binding of a protein

Howard Hughes Medical Institute, Program in Molecular Medicine, University of Massachusetts Medical Center, 373 Plantation Street, Suite 309, Worcester, MA 01605, USA.

*Present address: MBI Fermentas Inc., 7 Innovation Drive, Flamborough, ON, Canada L9H 7H9.
†To whom correspondence should be addressed. E-mail: michael.green@ummed.edu

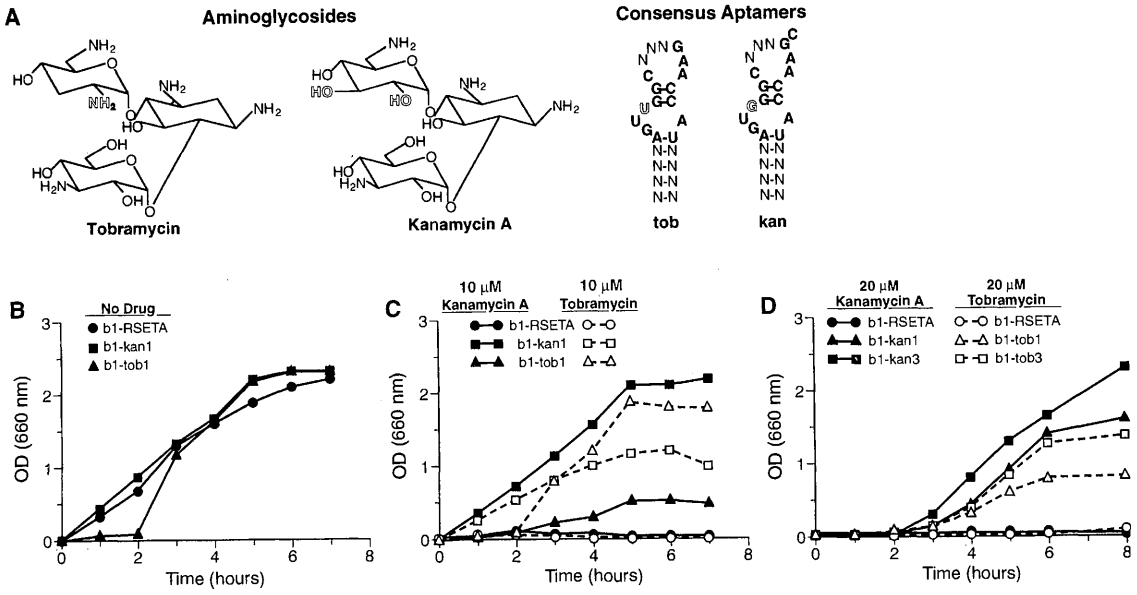

Fig. 1. Selective interaction between aminoglycosides and aminoglycoside aptamers in vivo. (**A**) Structures of aminoglycoside antibiotics and their aptamers. Consensus aptamers were identified after 10 to 12 rounds of selection. (**B** to **D**) Growth curves. Overnight cultures of *E. coli* BL-21 transformed with plasmids expressing RSETA, tob1, tob3, kan1, or kan3 were diluted 1:100 into medium containing the indicated concentration of aminoglycoside antibiotic. Optical density (660 nm) was measured at fixed intervals over 8 hours of growth at 37°C. (B) Growth in the absence of drug. (C) Growth in the presence of 10 μM kanamycin A or tobramycin. (D) Growth in the presence of 20 μM kanamycin A or tobramycin.